Clim. Past Discuss., 9, 4035–4063, 2013
www.clim-past-discuss.net/9/4035/2013/
doi:10.5194/cpd-9-4035-2013

Climate of the Past
Discussions
Open Access

Deglacial intermediate water reorganization: new evidence from the Indian Ocean

S. Romahn[1], **A. Mackensen**[1], **J. Groeneveld**[2], **and J. Pätzold**[2]

[1]Alfred-Wegener-Institut Helmholtz-Zentrum für Polar- und Meeresforschung, Am Alten Hafen 26, 27568 Bremerhaven, Germany
[2]MARUM-Center for Marine Environmental Sciences, Bremen University, Leobener Straße, 28359 Bremen, Germany

Received: 7 June 2013 – Accepted: 4 July 2013 – Published: 17 July 2013

Correspondence to: S. Romahn (sarah.romahn@awi.de)

Published by Copernicus Publications on behalf of the European Geosciences Union.

Abstract

The importance of intermediate water masses in climate change and ocean circulation has been emphasized recently. In particular, Antarctic Intermediate Water (AAIW) is thought to have acted as an active interhemispheric transmitter of climate anomalies. Here we reconstruct changes in AAIW signature and spatial and temporal evolution based on a 40 kyr time series of oxygen and carbon isotopes as well as planktic Mg/Ca based thermometry from a site in the western Indian Ocean. Our data suggest that AAIW transmitted Antarctic temperature trends to the equatorial Indian Ocean via the "oceanic tunnel" mechanism. Moreover, our results reveal that deglacial AAIW carried a signature of aged Southern Ocean deep water. We find no evidence of increased formation of intermediate waters during the deglaciation.

1 Introduction

Despite growing evidence that intermediate water masses originating from the Southern Hemisphere are an important component of the global thermohaline circulation, there is disagreement about the variability of chemical properties and the spatial dimension of these watermasses through time. Especially the architecture of the Southern Ocean's intermediate level during the last Termination is a matter of current debate. For example, an enhanced formation of AAIW during Heinrich event 1 (H1) and the Younger Dryas (YD) has been recorded in the Atlantic (Pahnke et al., 2008), in the Pacific (Pahnke and Zahn, 2005) and in the Indian Ocean (Jung et al., 2009).

AAIW is also thought to transmit climate anomalies from the Southern Ocean to the tropics, via the so-called "oceanic tunnel" (Liu and Yang, 2003; Ninnemann et al., 2006; Pena et al., 2013). This term describes the flow of southern-sourced waters via an intermediate pathway to the low latitude thermocline, where this extratropical water is supposed to regulate tropical sea surface temperature (SST). The growing number of high-resolution SST records from shallow depths of tropical oceans, showing an

CPD
9, 4035–4063, 2013

Antarctic-type SST pattern for the last deglaciation (Kiefer et al., 2006; Naidu and Govil, 2010; Visser et al., 2003; Weldeab et al., 2006), supports this idea and indicates that AAIW is elemental for interhemispheric forcing of climate variability.

In this context, the hypothesis that the deglacial atmospheric CO_2 increase and $\Delta^{14}C$ decline is explained by the release of carbon from an isolated deepwater carbon pool (Broecker, 1982), gained new attention. This idea has been corroborated recently since anomalous radiocarbon-depleted waters were identified in the Pacific (Marchitto et al., 2007; Sikes et al., 2000; Stott et al., 2009), the Atlantic (Keigwin, 2004; Robinson et al., 2005; Thornalley et al., 2011) and the Indian Ocean (Bryan et al., 2010). These old waters were all detected in thermocline to shallow intermediate depth and interpreted as pulses of preformed AAIW, and therewith locating the aged deep water reservoir in the Southern Ocean. Spero and Lea (2002) presented a superordinate hypothesis that interprets globally distributed carbon isotope minimum events (CIME, Ziegler et al., 2013) at glacial terminations as the result of increased upwelling of aged deep water in the Southern Ocean, once Antarctica began to warm and sea ice melted back. Accordingly, supersaturated deep waters emit CO_2, which results in rising CO_2 concentrations and decreasing $\delta^{13}C$ signature of the atmosphere, while the low $\delta^{13}C$ of these upwelled waters propagate northwards in AAIW and Subantarctic Mode Water (SAMW). The AAIW/SAMW $\delta^{13}C$ minimum, Antarctic temperature rise and atmospheric CO_2 rise coincide, because all these effects arise from the same process (Spero and Lea, 2002; Stephens and Keeling, 2000).

High-resolution sediment records from the tropical intermediate ocean are still rare, but they are essential to answer the questions of how the geographical and vertical extent of AAIW changed since the Last Glacial Maximum (LGM), and how AAIW influenced the physical properties of the tropical and subtropical oceans in both hemispheres, and therefore participated in interhemispheric forcing. Here we provide a new high-resolution time series of oxygen and carbon isotopes as well as planktic Mg/Ca based SST from the intermediate western Indian Ocean that spans the last 40 kyr to

CPD
9, 4035–4063, 2013

participate in the current discussion on the importance of AAIW/SAMW as part of the global overturning circulation.

2 Oceanographic framework

The study site GeoB12615-4 is located off Tanzania, East Africa (Fig. 1). It receives surface water predominantly from the westward flowing South Equatorial Current (SEC), to a large part supplied by the Indonesian Throughflow (Schott et al., 2009). Whereas SAMW from the southeast Indian Ocean is the source for thermocline waters, there are several sources that contribute to the intermediate waters of the Indian Ocean (Fine et al., 2008). Although You (1998) estimated the water along the western boundary at 5° N to be a mixture of 20 % AAIW, 70 % Red Sea Water, and 10 % Indonesian throughflow, Fine et al. (2008) found AAIW, entering the Indian Ocean from the southwest, to be the most significant ventilation source of the intermediate Indian Ocean, including the Arabian Sea. Both AAIW and SAMW are supposed to be open-ocean upwelled at 5–10° S due to Ekman divergence at the northern edge of the South Equatorial Counter Current (Schott and McCreary, 2001).

The formation of both AAIW and SAMW in the modern ocean is associated to the Subantarctic Front (SAF) at 45° to 55° S (Hartin et al., 2011; McCartney, 1977; Sloyan and Rintoul, 2001). In the past years, it has become common practice in paleoceanographic studies to refer to AAIW/SAMW when speaking of, in general, a glacial Southern component intermediate water, which originates from circumantarctic surface waters, subducts and subsequently spreads northwards (Bryan et al., 2010; Chen et al., 2011; Ninnemann and Charles, 1997; Spero and Lea, 2002). Although this is a simplification, it seems helpful when hypothesizing (schematically) about changes in Southern Ocean overturning (Marshall and Speer, 2012; Skinner et al., 2010). For the sake of clarity, we continue with this practice and refer to AAIW/SAMW subsequently in the text, always keeping in mind that this term represents southern component intermediate water as part of the Southern Ocean overturning circulation.

CPD
9, 4035–4063, 2013

3 Material and methods

3.1 Sampling

The gravity core GeoB12615-4 was recovered during Meteor cruise M75/2 in February 2008 at 07°08.30′ S 39°50.45′ W from 446 m water depth and spans 644 cm (Savoye et al., 2013). For this study we sampled at 4 cm spacing with a sample width of 1 cm. We wet sieved over 63 µm, 125 µm and 2 mm and dried the sediment fractions at 40 °C.

3.2 Age model

The chronology is based on 16 AMS (accelerator mass spectrometer) radiocarbon analyses, carried out at the Leibniz-Laboratory for Radiometric Dating and Isotope Research, Kiel. Both monospecific planktic foraminifera samples (*Globigerinoides ruber* white *s.s.*) and mixed samples of surface-dwelling planktic species (*Globigerinoides sacculifer*, *Globigerinella aequilateralis*, *Globigerinoides conglobatus*) were analysed. Measured radiocarbon ages were converted into calibrated ages before present (BP) using the Calib 6.0 software (Stuiver et al., 2005), based on the Marine09 calibration curve and a reservoir age correction of ΔR = 140 yr (Southon et al., 2002). The sedimentation rate varies strongly between the Holocene (average of 46 cm kyr^{-1}, highest beween ~ 8.7 and 8.2 kyr with 70 cm kyr^{-1}) and the glacial (below 10 cm kyr^{-1}). The complete dataset covers the past 40 kyr (Fig. 2).

3.3 Oxygen and carbon isotopes

For isotopic analysis, six to eight individuals of *G. ruber* white *s.s.* and three to four individuals of benthic foraminifer *Planulina ariminensis* were selected from the 250–300 µm fraction and from the total fraction, respectively. Isotope measurements were performed using Finnigan MAT 251 and MAT 253 isotope ratio mass spectrometers coupled to automatic carbonate preparation devices Kiel II and Kiel IV, respectively.

CPD
9, 4035–4063, 2013

Deglacial Intermediate Water reorganization

S. Romahn et al.

The isotope measurements were calibrated via NBS 19 international standard to the PDB scale. All results are given in δ-notation versus VPDB. Precision of measurements based on an internal laboratory standard (Solnhofen limestone) measured over a one-year period together with samples was better than 0.08 and 0.06 for oxygen and carbon isotopes, respectively

3.4 Mg/Ca ratios

35 to 45 individuals of *G. ruber* white *s.s.* (250–300 µm), were selected for Mg/Ca analysis of every second sample of the uppermost part of the core, resulting in a sampling interval of 8 cm. In contrast, in the lowermost 2.50 m of the core each sample was analysed (4 cm sampling interval). The shell samples were gently crushed and cleaned according to the cleaning protocol of Barker et al. (2003). Then the dissolved samples were centrifuged (10 min at 6000 rpm), transferred into autosampler tubes and diluted for analysis. Mg/Ca ratios were measured using a Perkin Elmer Optima 3300 R Inductively Coupled Plasma Optical Emission Spectrophotometer (ICP-OES) equipped with an auto sampler and an ultrasonic nebulizer U-5000 AT (Cetac Technologies Inc.) housed at the Faculty of Geosciences, University of Bremen. The Mg/Ca values are reported as mmol mol^{-1}. Instrumental precision was determined by analysis an external, in-house standard (Mg/Ca = 2.92 mmol mol^{-1}), which was measured after every fifth sample. The standard deviation of the external standard was ±0.48 %. Reproducibility of the samples (n = 14) was ±0.09 mmol mol^{-1}. Long-term measurement of an international limestone standard (ECRM752-1; Greaves et al., 2008) allows for interlaboratory comparison. Mn/Ca, Fe/Ca and Al/Ca were determined along with Mg/Ca because clay contamination of the foraminifera shells can affect the Mg/Ca ratios resulting in overestimated SST (Barker et al., 2003). Our results indicate no significant Mg contributions due to Mn-oxides, Mn-rich carbonates or clay contaminiation because average Mn/Ca, Fe/Ca and Al/Ca were < 0.1 mmol mol^{-1}. SSTs (T in °C) were calculated us-

ing the equation given by Anand et al. (2003):

$$\mathrm{Mg/Ca}\ (\mathrm{mmol\,mol^{-1}}) = 0.38\,\exp(0.090\,T) \tag{1}$$

4 Results

The δ^{18}O record of planktic *G. ruber* white *s.s.* (noted as $\delta^{18}O_p$) shifts between −0.25 ‰ during glacial conditions and −2.2 ‰ during the Holocene. The deglacial decline of $\delta^{18}O_p$ starts at 18.2 kyr and shows a clear setback to higher values at 13 kyr, which appears to resemble the Greenland ice cores and therefore Northern Hemisphere climate variability. In contrast, the stable isotope records of benthic *P. ariminensis* (noted as $\delta^{18}O_b$ and $\delta^{13}C_b$) and the SST record are out of phase with surface oxygen isotopes and resemble Antarctic climate variability. The $\delta^{18}O_b$ shifts between 2.5 ‰ in the LGM and ~ 1 ‰ for the Holocene. The record exhibits a deglacial decline starting at 19.5 kyr, and a slackening of $\delta^{18}O_b$ decrease during the Antarctic Cold Reversal (ACR). The record of surface carbon isotopes shows quite consistent values of 0.9–1.1 ‰ during the glacial, and an abrupt increase of about 0.7 ‰ during the early Holocene (EH), parallel to sea level rise, to ~ 1.4 ‰. The $\delta^{13}C_b$ varies around 1.5 ‰ between 35–18.2 kyr. Values decrease abruptly at 18.2 kyr (about 0.4 ‰), increase during the ACR and reach a minimum of 0.9 ‰ in the EH. Synchronous to the global sea level rise, $\delta^{13}C_b$ gradually increases about 0.5 ‰ to Holocene levels of approx. 1.5 ‰. The Mg/Ca based SST record exhibits a similar deglacial variability and shows a sudden temperature increase from ~ 25 °C to 27 °C at 18.2 kyr, an ACR-like temperature drop starting at 15 kyr, and a final increase to Holocene temperatures (28–29 °C) at around 13 kyr. To sum up; the $\delta^{18}O_p$ surface signal can be linked to Northern Hemisphere (NH) climate variability, whereas both the Mg/Ca based SST, as well as the $\delta^{18}O_b$ and $\delta^{13}C_b$ deep-water records are in line with Antarctic temperature records (Fig. 3).

CPD
9, 4035–4063, 2013

5 Discussion

5.1 Oceanic tunnel transmitting Antarctic temperature

It is a widespread feature of the Indian Ocean to show an Antarctic-style deglacial warming in surface-based temperature proxies (Govil and Naidu, 2010; Huguet et al., 2006; Levi et al., 2007), while surface δ^{18}O varies independently of SST reconstructions and likely reflects the influence of the monsoon (Anand et al., 2008; Huguet et al., 2006; Levi et al., 2007). On the contrary, benthic δ^{18}O records of intermediate depth carry a typical Antarctic signature (Anand et al., 2008; Jung et al., 2009; Lueckge et al., 2012). The idea that SST variability in the western Indian Ocean is controlled by Antarctic temperature via SAMW has been proposed by Kiefer et al. (2006) and was corroborated by Naidu and Govil (2010). The authors suggest the "oceanic tunnel" mechanism (Liu and Yang, 2003; Ninnemann et al., 2006), in form of SAMW that originates from subantarctic surface waters. After subducting and spreading northwards, SAMW returns to the surface in regions of equatorial upwelling and thus conveys surface water anomalies from the Subantarctic Zone to the tropical Indian Ocean. Here we confirm this interpretation by presenting a SST record from a location of modern AAIW/SAMW influence that clearly shows simultaneous warming of the tropical western Indian Ocean and Antarctica (Fig. 3). We find that our data necessarily call for an oceanic mechanism that modulated SST variability, for two reasons.

First, we can exclude that atmospheric processes controlled SST variability, because $\delta^{18}O_p$ of GeoB12615-4 with its distinct NH pattern differs so clearly from the SST data. This indicates two independent factors affect the surface water properties at our study site. Similarly, the Arabian Sea record NIOP905 (Huguet et al., 2006) exhibits an Antarctic-style SST pattern as well, evident in two independent surface temperature proxy reconstructions (TEX_{86} and alkenones), while the corresponding δ^{15}N record and planktic δ^{18}O follows NH climate variability. The δ^{15}N, a proxy for productivity changes, as well as planktic δ^{18}O likely reflect the strength of the Arabian Sea Sum-

CPD
9, 4035–4063, 2013

mer Monsoon (Ivanochko et al., 2005). If we conclude that our $\delta^{18}O_p$ reflects monsoon strength as well, and hence is controlled by an atmospheric process following NH climate, then SST variability following antarctic climate must be modulated differently. If atmospheric control can be ruled out, only oceanic control remains as a mechanism modulating SST.

Second, the benthic record of GeoB12615-4 does not only exhibit a $\delta^{18}O_b$ signal that is in phase with Antarctic temperature variability, it also shows a distinct carbon isotope minimum event (CIME) during the deglaciation (Ninnemann and Charles, 1997; Spero and Lea, 2002). This minimum is a common feature of both southern high latitude planktic $\delta^{13}C$ profiles (Bostock et al., 2004; Lopes dos Santos et al., 2012; Ninnemann and Charles, 1997; Pahnke and Zahn, 2005) and of tropical $\delta^{13}C$ records of subthermocline and intermediate depth (Curry and Oppo, 2005; Oppo and Fairbanks, 1989; Stott et al., 2009; Zahn and Stüber, 2002). Oppo and Fairbanks (1989) suggested CIME to be linked to AAIW/SAMW, and Lynch-Stieglitz et al. (1994) and Ninnemann and Charles (1997) assumed that CIME at sites ventilated by AAIW/SAMW reflect a preformed signal from Subantarctic surface waters. The combination of Antarctic-style benthic $\delta^{18}O$ and benthic $\delta^{13}C$ from site GeoB12615-4, showing a distinct deglacial minimum, confirms that the "oceanic tunnel" in form of AAIW/SAMW is the most likely mechanism controlling past SST in the western Indian Ocean.

5.2 AAIW/SAMW formation during the deglaciation

If SST variability is controlled by AAIW/SAMW, transmitting Antarctic temperature to the tropics, what in turn does the benthic $\delta^{13}C$ record tell us about AAIW/SAMW variability since glacial times? We first evaluate how the observed pattern in our benthic signal can be best explained by current concepts of deglacial $\delta^{13}C_{DIC}$ setting in the Southern Ocean.

CPD
9, 4035–4063, 2013

We then discuss how the spatial extent of AAIW/SAMW may have varied since the last glacial by combining our findings in the western Indian Ocean with recent data that focus on AAIW/SAMW variability as well.

5.2.1 Preformed δ^{13}C of deglacial AAIW/SAMW?

As described above, the globally distributed deglacial δ^{13}C minima (CIME) are consistently interpreted to reflect deep upwelling in the Southern Ocean and intermediate distribution of old, δ^{13}C depleted water (Spero and Lea, 2002). Moreover, findings of radiocarbon depleted intermediate waters have been reported from all oceans so far (Bryan et al., 2010; Mangini et al., 2010; Marchitto et al., 2007; Stott et al., 2009; Thornalley et al., 2011), but there are just as many results where no injections of old water could be found (Cléroux et al., 2011; De Pol-Holz et al., 2010, 2012; Rose et al., 2010; Sortor and Lund, 2011). If the strong depletion in radiocarbon was the result of increased upwelling of a long-time isolated carbon reservoir, it should stringently coincide with a δ^{13}C minimum of the same water mass, just as described by Spero and Lea (2002). This is the case for sites with pronounced radiocarbon depletions, such as off Baja California (Marchitto et al., 2007) and south of Iceland (Thornalley et al., 2010). This hypothesis also holds for the Indian Ocean, if we combine the results of Geob12615-4 and recently published ventilation age reconstructions in the Arabian Sea (Bryan et al., 2010). We compare $\delta^{13}C_b$ of GeoB12615-4 to intermediate water ventilation (Δ^{14}C (‰)), reconstructed from sediment cores RC27-14 and RC27-23, and see a remarkable similarity between the minima in our benthic carbon and highest values of intermediate water Δ^{14}C, especially when comparing to RC27-14 (596 m water depth) (Fig. 4). Whereas other ^{14}C anomalies, that are likely transmitted by AAIW/SAMW, indicate pulses of aged intermediate water during H1 and the Younger Dryas (Marchitto et al., 2007), the Arabian Sea records do not show high ventilation ages during YD. Instead, we see very large benthos–plankton differences and therefore the highest ventilation ages during the early Holocene (EH) in the Arabian Sea. This is exactly the same time interval when lowest $\delta^{13}C_b$ values are found in

GeoB12615-4. Additionally, the signals of core RC27-14 (596 m) and GeoB12615-4 (446 m), both monitoring a similar water depth, correlate more explicitly, which argues for a large-scale connection and a watermass like AAIW/SAMW to be the transmitter of both anomalies in the Indian Ocean. Therefore we conclude that the bottom signal of GeoB12615-4 reflects the deglacial evolution of the Southern Ocean and gives evidence of upwelled aged deep waters (Broecker, 1982) at high southern latitudes, which then flow northwards into all ocean basins as AAIW/SAMW.

5.2.2 CIME caused by temperature-dependent fractionation?

The carbon isotopic fractionation between atmosphere and ocean increases with decreasing temperature, with lower temperatures resulting in more enriched δ^{13}C values of dissolved inorganic carbon ($\delta^{13}C_{DIC}$) in seawater (Broecker and Maier-Reimer, 1992; Mackensen, 2008). Though there is no region where surface ocean carbon is in complete isotopic equilibrium with the atmosphere, the effects related to air–sea gas exchange play an important role in defining the surface $\delta^{13}C_{DIC}$, working in the opposite direction to the effect of biological cycling (Broecker and Maier-Reimer, 1992; Lynch-Stieglitz et al., 1995; Mackensen, 2012). Today, we find the highest $\delta^{13}C_{DIC}$ values of surface waters along the Subantarctic Front (SAF), between 45° to 55° S, because of low circumantarctic temperatures and enhanced air–sea gas exchange (Broecker and Maier-Reimer, 1992).

As the SST record and $\delta^{13}C_b$ (reflecting AAIW/SAMW) of GeoB12615-4 match so well during the deglaciation (Fig. 5), one could suggest that $\delta^{13}C_b$ and therefore $\delta^{13}C_{DIC}$ of AAIW/SAMW was simply the expression of temperature change at high southern latitudes, or in other words, the formation area of AAIW/SAMW: During the LGM, $\delta^{13}C_{DIC}$ of see-ice free surface seawater at high southern latitudes was high due to low temperatures and high wind speed. A deglacial temperature rise may have decreased the thermodynamic fractionation and therefore lead to lower values of surface $\delta^{13}C_{DIC}$, always tracing centennial-scale Antarctic temperatue variability. This signal

CPD
9, 4035–4063, 2013

was transferred to low latitudes as AAIW/SAMW almost time-invariant. In fact, if we assume 0.1 ‰ depletion of $\delta^{13}C_{DIC}$ per degree centigrade of cooling (Mook et al., 1974; Zhang et al., 1995), we would expect a $\delta^{13}C$ decrease of 0.35 ‰ for the deglaciation until the EH, and this comes close to the observed ∼ 0.5 ‰ shift in deglacial $\delta^{13}C_b$. Additionally, a displacement of the westerly wind belt (Lamy et al., 2004; Wyrwoll et al., 2000) may have reduced air–sea gas exchange of Southern Ocean surface waters, as proposed by Ninnemann and Charles (1997). According to this interpretation, deglacial $\delta^{13}C_b$ of GeoB12615-4 as well as the global ocurrence of CIME in shallow depth can be entirely explained by Southern Ocean surface water temperature variability and accordingly altered thermodynamic fractionation during air–sea CO_2 exchange at high latitudes, as originally proposed by Ninnemann and Charles (1997).

Indeed, based on our data alone we could reason that the deglacial CIME in our record is a purely temperature-dependent signal.

However, the corresponding radiocarbon depletions off Oman (Bryan et al., 2010) call for a mechanism that best explains the occurrence of both signals, CIME and radiocarbon depletions, detected in the same water mass; namely the mechanism proposed by Spero and Lea (2002). Nevertheless, since we cannot determine important prerequisites, such as the degree of equilibration between the surface ocean carbon and atmosphere, we do not want to definitely exclude that temperature-dependent fractionation during air–sea gas exchange played a role in developing deglacial CIME in AAIW/SAMW.

5.2.3 An additional atmospheric pathway for transmission of CIME?

The carbon isotope ratio of atmospheric CO_2 ($\delta^{13}C_{atm}$) experienced pronounced depletion during the deglaciation as well. New findings of $\delta^{13}C_{atm}$ (Schmitt et al., 2012) are likewise explained by the release of old carbon from the deep ocean, and in line with the concept drafted by Spero and Lea (2002). The high-resolution record shows $\delta^{13}C$ minima during H1 and YD, which is in line with the timing of the early H1-synchron

CPD
9, 4035–4063, 2013

CIME of many marine records, and also correlates with our benthic carbon isotope record (Fig. 6). Since a pronounced CIME without an associated radiocarbon depletion has been identified in intermediate waters off equatorial Africa (Cléroux et al., 2011), one has to consider that both signals needn't necessarily to be coupled, even though they may arise from the same process. In the Philippine Sea, western Pacific, the carbon isotope minimum is recorded in both surface and subsurface water, but with differing amplitude and timing. The independent signals are thought to be formed by atmospheric CO_2 imprint on the surface water in case of the surface signal, and via the "oceanic tunnel" and thus preformed AAIW in case of the subsurface one (Chen et al., 2011). So, the atmosphere can probably work as an additional pathway for transmitting the deglacial CIME to tropical oceans, which should be considered when interpreting deglacial $\delta^{13}C$ profiles. Comparing our data (Fig. 6) to the recent record of $\delta^{13}C_{atm}$ (Schmitt et al., 2012), the initial drop in both $\delta^{13}C_{atm}$ and $\delta^{13}C$ of AAIW/SAMW occurs synchronous and is of the same magnitude (approx. 0.3 ‰). However, since 12.3 kyr BP both records vary independently. This mismatch, along with the synchronous peaks of old carbon off Oman (Bryan et al., 2010), corroborates that the "oceanic tunnel" (Liu and Yang, 2003) mechanism is configuring the intermediate water history at our site.

5.2.4 Diminished or enhanced glacial AAIW/SAMW formation?

A current hypothesis proposes an enhanced production and northward flow of AAIW during H1 and YD in the Atlantic (Pahnke et al., 2008), the Pacific (Pahnke and Zahn, 2005) and in the Indian Ocean (Jung et al., 2009). For example, sediment core NIOP905 (1580 m) from the continental slope off Somalia (Fig. 7, see Fig. 1 for core location) shows an increase of benthic $\delta^{13}C$ during H1 and YD, which suggests intensified AAIW formation and inflow to the Indian Ocean (Jung et al., 2009). This is in line with results from the Pacific (MD97-2120, 1210 m, Pahnke and Zahn, 2005) and Atlantic Ocean (Pahnke et al., 2008), which also show higher benthic $\delta^{13}C$ and accordingly enhanced advection of AAIW during this time period. If we assume that deglacial AAIW/SAMW formed as proposed by Spero and Lea (2002), carrying pronounced CIME as a large-scale water mass signal, then our data contradict the interpretation of enhanced deglacial AAIW production (and subsequent inflow to the Arabian Sea), because both $\delta^{13}C$ datasets (NIOP905 and GeoB12615-4) anticorrelate during this specific time interval (H1 and YD) (Fig. 7). This apparent anticorrelation of carbon isotope signals within the intermediate stockwork was found in the South Pacific as well (Bostock et al., 2004), and it can even be found when using other water mass proxies, such as authigenic neodymium isotope ratios (ε_{Nd}) of seawater: two recent studies from the western tropical Atlantic present anticorrelating ε_{Nd} records from 546 m and 1330 m water depth, which potentially reflects reduced or even no contribution of deglacial AAIW in case of the shallow record, and enhanced advection of deglacial AAIW in case of the deeper one, respectively (Pahnke et al., 2008; Xie et al., 2012) – a contradiction which calls for an alternative interpretation of global intermediate water records that cover this particular time period. In general, the deglacial $\delta^{13}C$ minimum seems to be restricted to the surface and intermediate level down to approximately 800–900 m water depth both in the Indian Ocean and the Pacific, whereas the deglacial $\delta^{13}C$ increase, consistently interpreted as "enhanced" flow of AAIW, characterizes the lower intermediate level of 1000–1500 m water depth, such as recorded in NIOP905 or MD97-2120, respectively. Furthermore, the upper water level is mostly associated to the radiocarbon depletion, whereas the lower level, showing the $\delta^{13}C$ maximum, gives no evidence of anomalous high ventilation ages (Rose et al., 2010). Bryan et al. (2011) suggest a deglacial boundary shift between AAIW and Circumpolar Deep Water (CDW), as ventilation age reconstructions in the Pacific Ocean at 1032 m water depth show much older glacial waters and a deglacial increase in $\Delta^{14}C$. Consequently, the missing signature of old carbon in some intermediate records can only be explained by the fact that the chosen core site is located "too deep" (1000 m and greater water depth) and does not catch deglacial AAIW/SAMW.

Transferring this idea to the Arabian Sea, we suggest $\delta^{13}C_b$ of NIOP905 does not record AAIW/SAMW at any time. Instead, benthic $\delta^{13}C$ of NIOP905 seems to record a watermass that is unaffected of the specific upwelling processes in the deglacial

Southern Ocean, that lead to both CIME and strong radiocarbon depletions in southern component intermediate waters. It rather resembles the $\delta^{13}C_b$ pattern observed in mid-depth South Atlantic (Ziegler et al., 2013), representing one part of the "mid-depth overturning circuit" in the Southern Ocean. Hence we suggest that the benthic record of NIOP905 as well as those of other "deeper" intermediate sites, such as MD97-2120 (Pahnke and Zahn, 2005) and GC-12 (Bostock et al., 2004) from the Pacific, might record a deglacial analogue of modern CDW predominantly, as part of the Southern Ocean overturning (Skinner et al., 2010; Ziegler et al., 2013). Particularly higher $\delta^{13}C$ values of deglacial CDW might result from changing endmember compositions (Curry and Oppo, 2005) in the deep Southern Ocean, and this is how we interpret the pattern observed in benthic records of "deeper" intermediate sites. The fact that glacial–interglacial changes in Southern Ocean overturning circulation most likely result in changing water mass signatures has to be taken into account when interpreting deglacial $\delta^{13}C$ profiles. Moreover, considering the concept that preformed $\delta^{13}C$ determined the signature of deglacial AAIW/SAMW, we suggest that AAIW/SAMW convection was restricted down to approx. 800–900 m, whereas the lower intermediate levels were filled by a southern-sourced water analogue to modern CDW.

6 Conclusions

In this study we present evidence that deglacial SST variability in the western Indian Ocean is primarily controlled by Antarctic air temperature, which was transmitted to the equatorial Indian Ocean on a subsurface pathway by AAIW/SAMW. We discuss current concepts of what determines the deglacial AAIW/SAMW $\delta^{13}C$ signature, and we support the hypothesis (Spero and Lea, 2002) that deglacial upwelling of isolated Southern Ocean deep water caused a drop in atmospheric, surface and subsurface ocean carbon isotopy (CIME) and thereby determines the AAIW/SAMW signature recorded at our study site.

CPD
9, 4035–4063, 2013

Moreover, we discuss whether recent carbon isotope records of the intermediate ocean give evidence of enhanced AAIW/SAMW flow during H1 and YD, but we do not find that deglacial AAIW/SAMW formation was enhanced. Instead, we suggest that AAIW/SAMW convection depth was shallower than today, whereas the deeper intermediate levels (> 1000 m) were filled by southern-sourced water analogue to modern CDW. Finally, the question remains unanswered why Indian Ocean AAIW/SAMW shows a pronounced CIME and corresponding radiocarbon minimum (Bryan et al., 2011) during the EH, while other regional (Marchitto et al., 2007) and global records (Schmitt et al., 2012) precede.

Acknowledgements. We thank Günther Meyer, Heike Röben, Lisa Schönborn, Susanne Wiebe for help and advice in the laboratories, as well as the ship crew and scientific parties of Meteor cruise M75/2. We also thank Franziska Kersten and Johannes Ullermann for essential discussion and comments. This work was funded by the Deutsche Forschungsgemeinschaft (DFG) as part of the DFG-Research Center/Cluster of Excellence MARUM "The Ocean in the Earth System".

References

Anand, P., Elderfield, H., and Conte, M. H.: Calibration of Mg/Ca thermometry in planktonic foraminifera from a sediment trap time series, Paleoceanography, 18, PA1050, doi:10.1029/2002PA000846, 2003.

Anand, P., Kroon, D., Singh, A. D., Ganeshram, R. S., Ganssen, G., and Elderfield, H.: Coupled sea surface temperature–seawater δ^{18}O reconstructions in the Arabian Sea at the millennial scale for the last 35 ka, Paleoceanography, 23, PA4207, doi:10.1029/2007PA001564, 2008.

Andersen, K. K., Azuma, N., Barnola, J.-M., Bigler, M., Biscaye, P., Caillon, N., Chappellaz, J., Clausen, H. B., Dahl-Jensen, D., and Fischer, H.: High-resolution record of Northern Hemisphere climate extending into the last interglacial period, Nature, 431, 147–151, 2004.

Barker, S., Greaves, M., and Elderfield, H.: A study of cleaning procedures used for foraminiferal Mg/Ca paleothermometry, Geochem. Geophy. Geosy., 4, 8407, doi:10.1029/2003GC000559, 2003.

Bostock, H. C., Opdyke, B. N., Gagan, M. K., and Fifield, L. K.: Carbon isotope evidence for changes in Antarctic Intermediate Water circulation and ocean ventilation in the southwest Pacific during the last deglaciation, Paleoceanography, 19, PA4013, doi:10.1029/2004PA001047, 2004.

Broecker, W.: Glacial to interglacial changes in ocean chemistry, Prog. Oceanogr., 11, 151–197, 1982.

Broecker, W. S. and Maier-Reimer, E.: The influence of air and sea exchange on the carbon isotope distribution in the sea, Global Biogeochem. Cy., 6, 315–320, 1992.

Bryan, S., Lehman, S., Marchitto, T., and Ninnemann, U.: Intermediate Water Radiocarbon Anomalies During the Last Deglaciation, AGU Fall Meeting, San Francisco, California, USA, 5–9 December 2011, PP23E-02, 2006.

Bryan, S. P., Marchitto, T. M., and Lehman, S. J.: The release of ^{14}C-depleted carbon from the deep ocean during the last deglaciation: evidence from the Arabian Sea, Earth Planet. Sc. Lett., 298, 244–254, 2010.

Chen, S. X., Li, T. G., Tang, Z., Qiu, X. H., Xiong, Z. F., Nan, Q. Y., Xu, Z. K., and Chang, F. M.: Response of the northwestern Pacific upper water δ^{13}C to the last deglacial ventilation of the deep Southern Ocean, Chinese Sci. Bull., 56, 2628–2634, 2011.

Cléroux, C., deMenocal, P., and Guilderson, T.: Deglacial radiocarbon history of tropical Atlantic thermocline waters: absence of CO_2 reservoir purging signal, Quaternary Sci. Rev., 30, 1875–1882, 2011.

Curry, W. B. and Oppo, D. W.: Glacial water mass geometry and the distribution of δ^{13}C of ΣCO_2 in the western Atlantic Ocean, Paleoceanography, 20, PA1017, doi:10.1029/2004PA001021, 2005.

De Pol-Holz, R., Keigwin, L., Southon, J., Hebbeln, D., and Mohtadi, M.: No signature of abyssal carbon in intermediate waters off Chile during deglaciation, Nat. Geosci., 3, 192–195, 2010.

De Pol-Holz, R., Mohtadi, M., and Southon, J.: Intermediate water radiocarbon off west Sumatra during the last 45 000 years, EGU General Assembly, Vienna, Austria, 22–27 April 2012, EGU2012-11829, 2012.

Fine, R. A., Smethie Jr., W. M., Bullister, J. L., Rhein, M., Min, D.-H., Warner, M. J., Poisson, A., and Weiss, R. F.: Decadal ventilation and mixing of Indian Ocean waters, Deep-Sea Res. Pt. I, 55, 20–37, 2008.

CPD
9, 4035–4063, 2013

Deglacial Intermediate Water reorganization

S. Romahn et al.

Govil, P. and Naidu, P. D.: Evaporation–precipitation changes in the eastern Arabian Sea for the last 68 ka, implications on monsoon variability, Paleoceanography, 25, PA1210, doi:10.1029/2008PA001687, 2010.
Greaves, M., Caillon, N., Rebaubier, H., Bartoli, G., Bohaty, S., Cacho, I., Clarke, L., Cooper, M., Daunt, C., and Delaney, M.: Interlaboratory comparison study of calibration standards for foraminiferal Mg/Ca thermometry, Geochem. Geophy. Geosy., 9, Q08010, doi:10.1029/2008GC001974, 2008.
Hartin, C. A., Fine, R. A., Sloyan, B. M., Talley, L. D., Chereskin, T. K., and Happell, J.: Formation rates of Subantarctic mode water and Antarctic intermediate water within the South Pacific, Deep-Sea Res. Pt. I, 58, 524–534, 2011.
Huguet, C., Kim, J. H., Damsté, J. S. S., and Schouten, S.: Reconstruction of sea surface temperature variations in the Arabian Sea over the last 23 kyr using organic proxies (TEX86 and UK37), Paleoceanography, 21, PA3003, doi:10.1029/2005PA001215, 2006.
Ivanochko, T. S., Ganeshram, R. S., Brummer, G.-J. A., Ganssen, G., Jung, S. J., Moreton, S. G., and Kroon, D.: Variations in tropical convection as an amplifier of global climate change at the millennial scale, 235, 302–314, doi:10.1016/j.epsl.2005.04.002, 2005.
Jouzel, J., Masson-Delmotte, V., Cattani, O., Dreyfus, G., Falourd, S., Hoffmann, G., Minster, B., Nouet, J., Barnola, J.-M., and Chappellaz, J.: Orbital and millennial Antarctic climate variability over the past 800 000 years, Science, 317, 793–796, 2007.
Jung, S. J. A., Kroon, D., Ganssen, G., Peeters, F., and Ganeshram, R.: Enhanced Arabian Sea intermediate water flow during glacial North Atlantic cold phases, Earth Planet. Sc. Lett., 280, 220–228, 2009.
Keigwin, L. D.: Radiocarbon and stable isotope constraints on Last Glacial Maximum and Younger Dryas ventilation in the western North Atlantic, Paleoceanography, 19, PA4012, doi:10.1029/2004PA001029, 2004.
Kiefer, T., McCave, I. N., and Elderfield, H.: Antarctic control on tropical Indian Ocean sea surface temperature and hydrography, Geophys. Res. Lett., 33, L24612, doi:10.1029/2006GL027097, 2006.
Lamy, F., Kaiser, J., Ninnemann, U., Hebbeln, D., Arz, H. W., and Stoner, J.: Antarctic timing of surface water changes off Chile and Patagonian ice sheet response, Science, 304, 1959–1962, 2004.
Levi, C., Labeyrie, L., Bassinot, F., Guichard, F., Cortijo, E., Waelbroeck, C., Caillon, N., Duprat, J., de Garidel-Thoron, T., and Elderfield, H.: Low-latitude hydrological cycle and

rapid climate changes during the last deglaciation, Geochem. Geophy. Geosy., 8, Q05N12, doi:10.1029/2006GC001514, 2007.
Liu, Z. and Yang, H.: Extratropical control of tropical climate, the atmospheric bridge and oceanic tunnel, Geophys. Res. Lett, 30, 1230, doi:10.1029/2002GL016492, 2003.
Lopes dos Santos, R. A., Wilkins, D., De Deckker, P., and Schouten, S.: Late Quaternary productivity changes from offshore Southeastern Australia: a biomarker approach, Palaeogeogr. Palaeocl., 363–364, 48–56, 2012.
Lueckge, A., Deplazes, G., Stuut, J. B., Pätzold, J., Kuhlmann, H., Scheeder, G., and Haug, G.: Monsoonal and oceanographic variability in the Arabian Sea during the last glacial period, AGU Fall Meeting, San Francisco, California, USA, 3–7 December 2012, PP52A-07, 2012.
Lynch-Stieglitz, J., Fairbanks, R. G., and Charles, C. D.: Glacial–interglacial history of Antarctic Intermediate Water: relative strengths of Antarctic versus Indian Ocean sources, Paleoceanography, 9, PA729, doi:10.1029/93PA02446, 1994.
Lynch-Stieglitz, J., Stocker, T. F., Broecker, W. S., and Fairbanks, R. G.: The influence of air–sea exchange on the isotopic composition of oceanic carbon: observations and modeling, Global Biogeochem. Cy., 9, 653–665, 1995.
Mackensen, A.: On the use of benthic foraminiferal δ^{13}C in palaeoceanography: constraints from primary proxy relationships, Geol. Soc. Lond. Spec. Pub., 303, 121–133, 2008.
Mackensen, A.: Strong thermodynamic imprint on recent bottom-water and epibenthic δ^{13}C in the Weddell Sea revealed: implications for glacial Southern Ocean ventilation, Earth Planet. Sc. Lett., 317–318, 20–26, 2012.
Mangini, A., Godoy, J., Godoy, M., Kowsmann, R., Santos, G., Ruckelshausen, M., Schroeder-Ritzrau, A., and Wacker, L.: Deep sea corals off Brazil verify a poorly ventilated Southern Pacific Ocean during H2, H1 and the Younger Dryas, Earth Planet. Sc. Lett., 293, 269–276, 2010.
Marchitto, T. M., Lehman, S. J., Ortiz, J. D., Flückiger, J., and van Geen, A.: Marine radiocarbon evidence for the mechanism of deglacial atmospheric CO_2 rise, Science, 316, 1456–1459, 2007.
Marshall, J. and Speer, K.: Closure of the meridional overturning circulation through Southern Ocean upwelling, Nat. Geosci., 5, 171–180, 2012.
McCartney, M. S.: Subantarctic Mode Water, A Voyage of Discovery: George Deacon 70th Anniversary Volume, Supplement to Deep-Sea Research, edited by: Angel, M. V., Pergamon Press, Oxford, 103–119, 1977.

CPD
9, 4035–4063, 2013
Deglacial Intermediate Water reorganization
S. Romahn et al.

Mook, W., Bommerson, J., and Staverman, W.: Carbon isotope fractionation between dissolved bicarbonate and gaseous carbon dioxide, Earth Planet. Sc. Lett., 22, 169–176, 1974.
Naidu, P. D. and Govil, P.: New evidence on the sequence of deglacial warming in the tropical Indian Ocean, J. Quaternary Sci., 25, 1138–1143, 2010.
Ninnemann, U. S. and Charles, C. D.: Regional differences in Quaternary Subantarctic nutrient cycling: link to intermediate and deep water ventilation, Paleoceanography, 12, 560–567, 1997.
Ninnemann, U. S., Kleiven, H., and Euler, C.: Covariation in SE Pacific surface and intermediate water properties on centennial–millennial timescales-constraints on the role of the "oceanic tunnel" in abrupt climate change, EGU General Assembly, Vienna, Austria, 2–7 April 2006, EGU06-A-11008, 2006.
Oppo, D. W. and Fairbanks, R. G.: Carbon isotope composition of tropical surface water during the past 22 000 years, Paleoceanography, 4, 333–351, 1989.
Pahnke, K. and Zahn, R.: Southern Hemisphere water mass conversion linked with North Atlantic climate variability, Science, 307, 1741–1746, 2005.
Pahnke, K., Goldstein, S. L., and Hemming, S. R.: Abrupt changes in Antarctic Intermediate Water circulation over the past 25 000 years, Nat. Geosci., 1, 870–874, 2008.
Pena, L., Goldstein, S., Hemming, S., Jones, K., Calvo, E., Pelejero, C., and Cacho, I.: Rapid changes in meridional advection of Southern Ocean intermediate waters to the tropical Pacific during the last 30 kyr, Earth Planet. Sc. Lett., 368, 20–32, 2013.
Robinson, L. F., Adkins, J. F., Keigwin, L. D., Southon, J., Fernandez, D. P., Wang, S., and Scheirer, D. S.: Radiocarbon variability in the western North Atlantic during the last deglaciation, Science, 310, 1469–1473, 2005.
Rose, K. A., Sikes, E. L., Guilderson, T. P., Shane, P., Hill, T. M., Zahn, R., and Spero, H. J.: Upper-ocean-to-atmosphere radiocarbon offsets imply fast deglacial carbon dioxide release, Nature, 466, 1093–1097, 2010.
Savoye, B., Ridderinkhof, H., Pätzold, J., and Schneider, R.: Western Indian Ocean Climate and Sedimentation, Cruise No. M75, 29 December 2007–April, 2008, Port Louis (Mauritius)–Cape Town (South Africa), METEOR-Berichte, 196, 2013.
Schmitt, J., Schneider, R., Elsig, J., Leuenberger, D., Lourantou, A., Chappellaz, J., Köhler, P., Joos, F., Stocker, T. F., and Leuenberger, M.: Carbon isotope constraints on the deglacial CO_2 rise from ice cores, Science, 336, 711–714, 2012.

CPD
9, 4035–4063, 2013

Title Page
Abstract Introduction
Conclusions References
Tables Figures
◂◂ ▸▸
◂ ▸
Back Close
Full Screen / Esc
Printer-friendly Version
Interactive Discussion

Schott, F. A. and McCreary, J. P.: The monsoon circulation of the Indian Ocean, Prog. Oceanogr., 51, 1–123, 2001.
Schott, F. A., Dengler, M., and Schoenefeldt, R.: The shallow overturning circulation of the Indian Ocean, Prog. Oceanogr., 53, 57–103, 2002.
Schott, F. A., Xie, S.-P., and McCreary Jr., J. P.: Indian Ocean circulation and climate variability, Rev. Geophys., 47, RG1002, doi:10.1029/2007RG000245, 2009.
Sikes, E. L., Samson, C. R., Guilderson, T. P., and Howard, W. R.: Old radiocarbon ages in the southwest Pacific Ocean during the last glacial period and deglaciation, Nature, 405, 555–559, 2000.
Skinner, L., Fallon, S., Waelbroeck, C., Michel, E., and Barker, S.: Ventilation of the deep Southern Ocean and deglacial CO_2 rise, Science, 328, 1147–1151, 2010.
Sloyan, B. M. and Rintoul, S. R.: Circulation, renewal, and modification of Antarctic Mode and Intermediate Water, J. Phys. Oceanogr., 31, 1005–1030, 2001.
Sortor, R. N. and Lund, D. C.: No evidence for a deglacial intermediate water $\Delta^{14}C$ anomaly in the SW Atlantic, Earth Planet. Sc. Lett., 310, 65–72, 2011.
Southon, J., Kashgarian, M., Fontugne, M., Metivier, B., and Yim, W. W. S.: Marine reservoir corrections for the Indian Ocean and Southeast Asia, Radiocarbon, 44, 167–180, 2002.
Spero, H. J. and Lea, D. W.: The cause of carbon isotope minimum events on glacial terminations, Science, 296, 522–525, 2002.
Stephens, B. B. and Keeling, R. F.: The influence of Antarctic sea ice on glacial–interglacial CO_2 variations, Nature, 404, 171–174, 2000.
Stott, L., Southon, J., Timmermann, A., and Koutavas, A.: Radiocarbon age anomaly at intermediate water depth in the Pacific Ocean during the last deglaciation, Paleoceanography, 24, PA2223, doi:10.1029/2008PA001690, 2009.
Thornalley, D. J. R., Elderfield, H., and McCave, I. N.: Intermediate and deep water paleoceanography of the northern North Atlantic over the past 21 000 years, Paleoceanography, 25, PA1211, doi:10.1029/2009PA001833, 2010.
Thornalley, D. J. R., Barker, S., Broecker, W. S., Elderfield, H., and McCave, I. N.: The deglacial evolution of North Atlantic deep convection, Science, 331, 202–205, 2011.
Visser, K., Thunell, R., and Stott, L.: Magnitude and timing of temperature change in the Indo-Pacific warm pool during deglaciation, Nature, 421, 152–155, 2003.

CPD
9, 4035–4063, 2013

Weldeab, S., Schneider, R. R., and Kölling, M.: Deglacial sea surface temperature and salinity increase in the western tropical Atlantic in synchrony with high latitude climate instabilities, Earth Planet. Sc. Lett., 241, 699–706, 2006.

Wyrwoll, K.-H., Dong, B., and Valdes, P.: On the position of Southern Hemisphere westerlies at the Last Glacial Maximum: an outline of AGCM simulation results and evaluation of their implications, Quaternary Sci. Rev., 19, 881–898, 2000.

Xie, R. C., Marcantonio, F., and Schmidt, M. W.: Deglacial variability of Antarctic Intermediate Water penetration into the North Atlantic from authigenic neodymium isotope ratios, Paleoceanography, 27, PA3221, doi:10.1029/2012PA002337, 2012.

You, Y.: Intermediate water circulation and ventilation of the Indian Ocean derived from water-mass contributions, J. Mar. Res., 56, 1029–1067, 1998.

Zahn, R. and Stüber, A.: Suborbital intermediate water variability inferred from paired benthic foraminiferal Cd/Ca and $\delta^{13}C$ in the tropical West Atlantic and linking with North Atlantic climates, Earth Planet. Sc. Lett., 200, 191–205, 2002.

Zhang, J., Quay, P., and Wilbur, D.: Carbon isotope fractionation during gas–water exchange and dissolution of CO_2, Geochim. Cosmochim. Ac., 59, 107–114, 1995.

Ziegler, M., Diz, P., Hall, I. R., and Zahn, R.: Millennial-scale changes in atmospheric CO_2 levels linked to the Southern Ocean carbon isotope gradient and dust flux, Nat. Geosci., 6, 457–461, 2013.

CPD
9, 4035–4063, 2013

Deglacial Intermediate Water reorganization

S. Romahn et al.

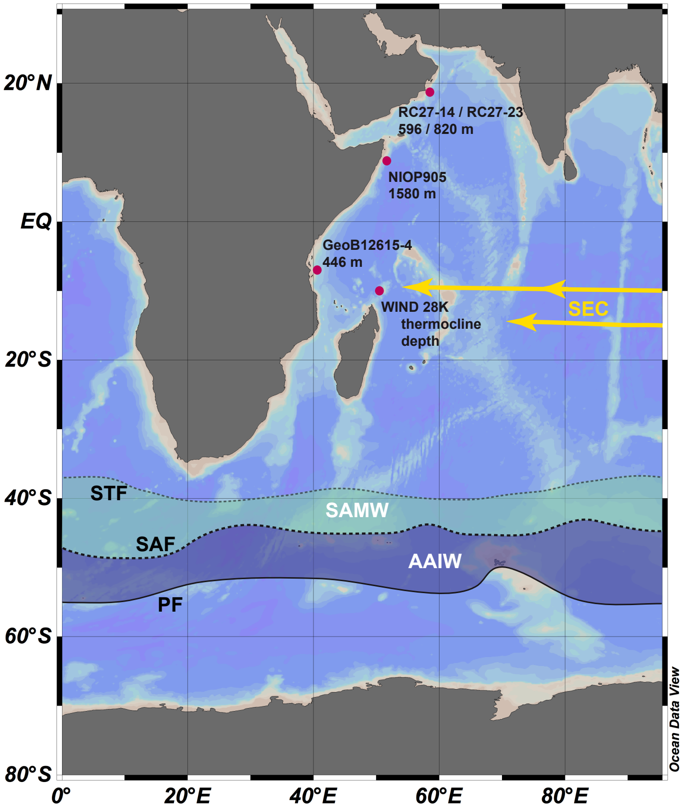

Fig. 1. Location map of sediment core records from the Indian Ocean discussed in this paper. Oman cores RC27-14 and RC27-23 (Bryan et al., 2010), Somalia core NIOP905 (Jung et al., 2009), Tanzania core GeoB12615-4 (this study) and Madagascar core WIND28K (Kiefer et al., 2006). Hydrographic fronts, and formation area of Intermediate water masses: STF: Subtropical Front; SAF: Subantarctic Front; PF: Polar Front; SAMW: Subantarctic Mode Water; AAIW: Antarctic Intermediate Water. Redrawn after (Pena et al., 2013; Schott et al., 2002).

CPD
9, 4035–4063, 2013

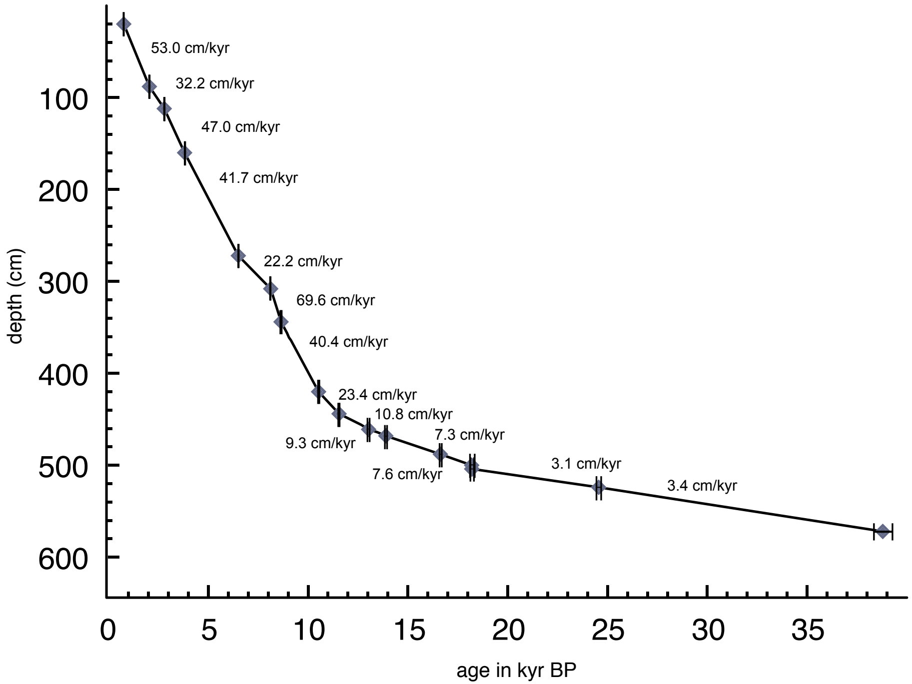

Fig. 2. Age–depth relationship of core GeoB12615-4, including linear sedimentation rates and calibrated radiocarbon ages with error bars

CPD
9, 4035–4063, 2013

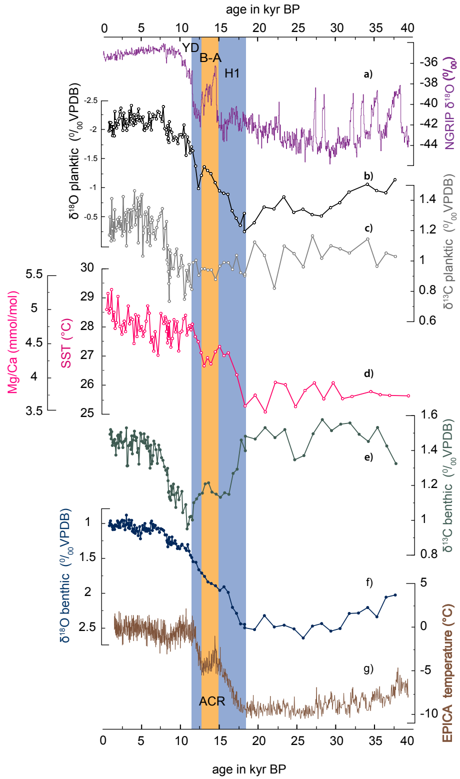

Fig. 3. Comparison of ice core records with data of GeoB12615-4 spanning the last 40 kyr. **(a)** NGRIP stable oxygen isotopic record (Andersen et al., 2004). **(b)** $\delta^{18}O_{planktic}$ record of GeoB12615-4 in ‰ VPDB. **(c)** $\delta^{13}C_{planktic}$ record of GeoB12615-4 in ‰ VPDB. **(d)** Shell Mg/Ca ratio of planktic foraminifera in mmol mol^{-1} and reconstructed SST record of GeoB12615-4 in °C. **(e)** $\delta^{13}C_{benthic}$ record of GeoB12615-4 in ‰ VPDB. **(f)** $\delta^{18}O_{benthic}$ record of GeoB12615-4 in ‰ VPDB. **(g)** EPICA Dome C ice core temperature estimates (Jouzel et al., 2007).

CPD
9, 4035–4063, 2013

Title Page
Abstract | Introduction
Conclusions | References
Tables | Figures
◂| |▸
◂ ▸
Back | Close
Full Screen / Esc
Printer-friendly Version
Interactive Discussion

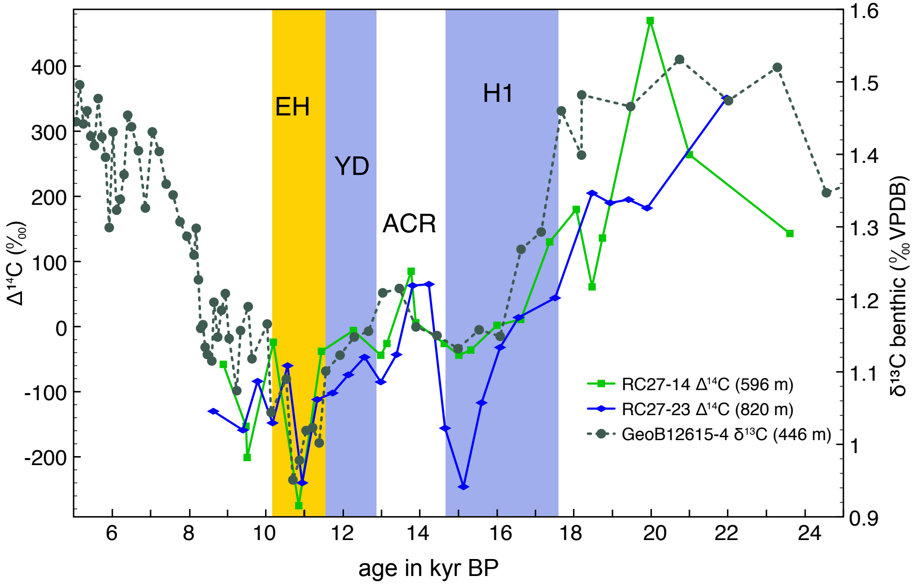

Fig. 4. Comparison of GeoB12615-4 and sediment records from the Arabian Sea. GeoB12615-4: $\delta^{13}C_{benthic}$ record in ‰ VPDB (green). Arabian Sea RC27-14 and RC27-23: intermediate water $\Delta^{14}C$ as a measure for ventilation age.

CPD
9, 4035–4063, 2013

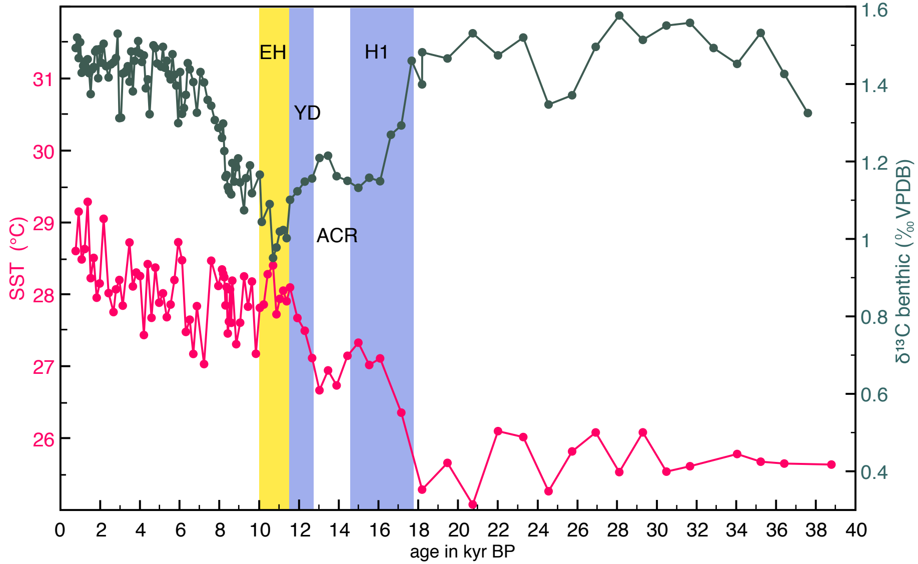

Fig. 5. Comparison of $\delta^{13}C_{benthic}$ record in ‰ VPDB (green) and SST record based on shell Mg/Ca ratio of planktic foraminifera in °C (pink) of GeoB12615-4. EH, YD, ACR and H1 indicate Early Holocene, Younger Dryas, Antarctic Cold Reversal and Heinrich event 1, respectively.

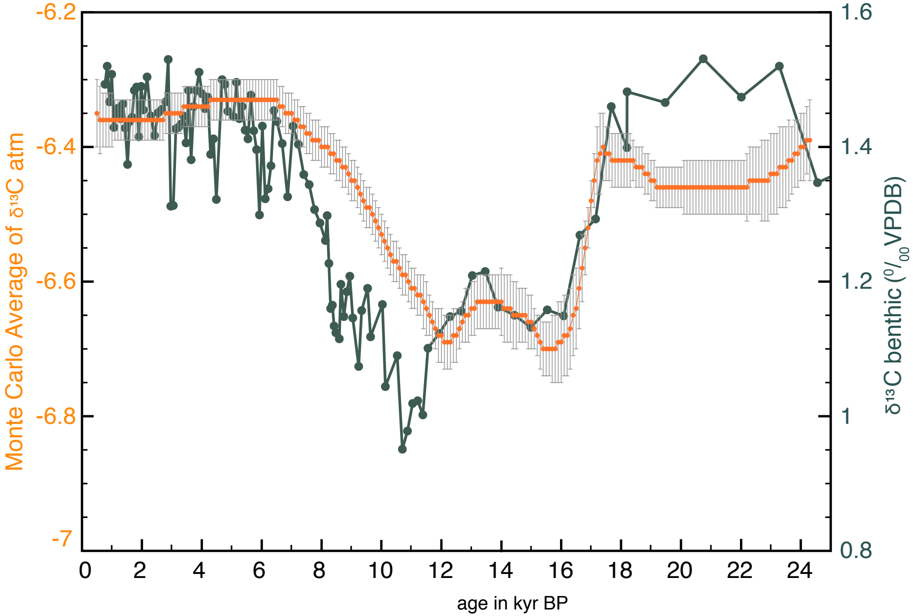

Fig. 6. Comparison of benthic carbon isotope record of GeoB12615-4 in ‰ VPDB (green) and Ice core reconstructions of atmospheric $\delta^{13}C$ ($\delta^{13}C_{atm}$) for the last 24 kyr (yellow, Schmitt et al., 2012).

CPD
9, 4035–4063, 2013

Deglacial Intermediate Water reorganization

S. Romahn et al.

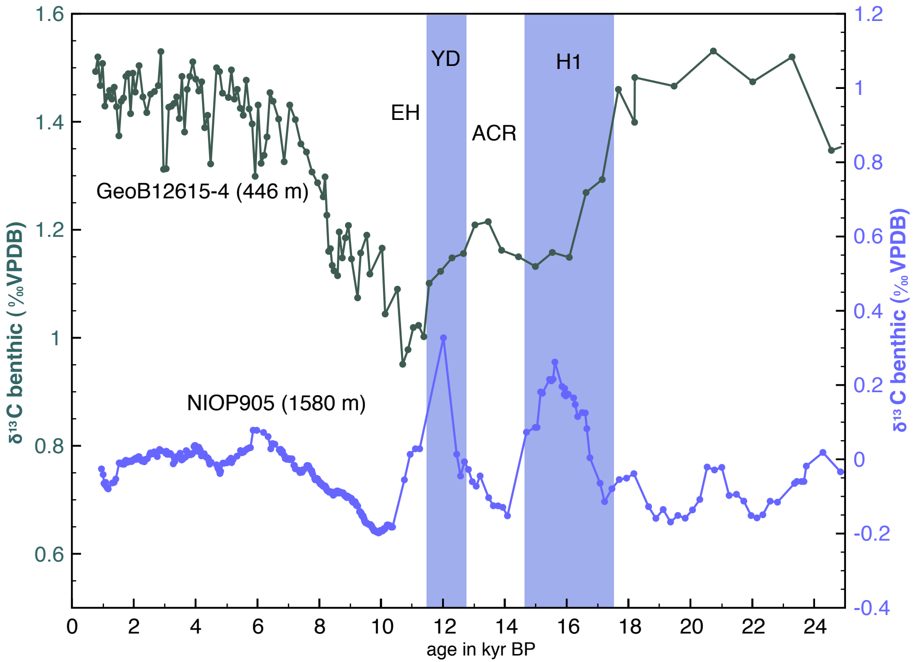

Fig. 7. Comparison of benthic carbon isotope records. GeoB12615-4 (green) and NIOP905 (purple). For core position see Fig. 1.

CPD
9, 4035–4063, 2013

Deglacial Intermediate Water reorganization

S. Romahn et al.